Jurnal Teknologi

Full Paper

BIS(BIPYRIDYL)-RU(II)-1-BENZOYL-3-(PYRIDINE-2-YL)-1H-PYRAZOLE AS POTENTIAL PHOTOSENSITISER: EXPERIMENTAL AND DENSITY FUNCTIONAL THEORY STUDY

Wun-Fui Mark-Lee[a], Febdian Rusydi[b], Lorna Jeffery Minggu[c], Takashi Kubo[d], Mohammad Kassim[a,c*]

[a]School of Chemical Sciences and Food Technology, Faculty of Science and Technology, Universiti Kebangsaan Malaysia, Selangor, Malaysia
[b]Department of Physics, Faculty of Science and Technology, University of Airlangga, Jl. Mulyorejo, Surabaya, Indonesia.
[c]Fuel Cell Institute, Universiti Kebangsaan Malaysia, Selangor, Malaysia
[d]Department of Chemistry, Graduate School of Science, Osaka University, Toyonaka, Osaka, Japan

Article history
Received
17 October 2015
Received in revised form
3 July 2016
Accepted
16 July 2016

*Corresponding author
mb_kassim@ukm.edu.my

Graphical abstract

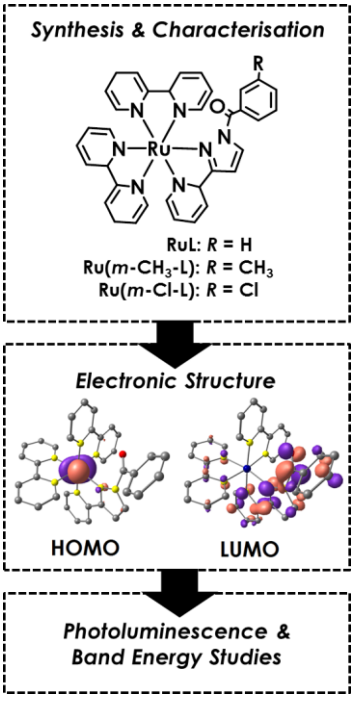

Abstract

Ru(II) complexes, $[Ru(bpy)_2(m\text{-}R\text{-}L)](PF_6)_2$ where bpy = 2,2'-bipyridyl and *m-R*-L= 1-(*meta-R*)-benzoyl-3-(pyridine-2-yl)-1H-pyrazole derivatives (*R* = H, CH_3 and Cl) abbreviated as RuL, Ru(*m*-CH_3-L) and Ru(*m*-Cl-L) complexes, respectively, were synthesized and characterized with spectroscopic techniques namely, infrared, UV-Vis and nuclear magnetic resonance (NMR), photoluminescence and mass spectroscopy. Density functional theory (DFT) and time-dependent (TD) DFT calculations were carried out to study the structural and electronic features of the molecules. These Ru(II) complexes exhibit photo-electronic properties required for a photosensitiser in a TiO_2-catalysed photoelectrochemical (PEC) cell. In-depth understanding of the *R*-L fragment functionality is important to tune the photo-electronic properties of the Ru(II) complex. The highest-occupied molecular orbital (HOMO) is mainly localized at the Ru(II) centre, while the LUMO is dominantly spread across the *R*-L ligand. The Ru(II) complexes showed favourable metal-to-ligand charge transfer (MLCT) energy levels, which are comparably higher than the conduction band of TiO_2 to facilitate electron injection process. Among the Ru(II) complexes, Ru(*m*-Cl-L) comparatively possesses the highest photoluminescence quantum yield and has the potential to be applied as photosensitiser in PEC systems.

Keywords: 1-benzoyl-3-(pyridine-2-yl)-1H-pyrazole, DFT, photoluminescence, Ru(II) photosensitiser, photoelectrochemical

© 2017 Penerbit UTM Press. All rights reserved

1.0 INTRODUCTION

The research on diimine compound that acts as a bidentate ligand through *NN* donor atoms such as pyridine-pyrazole (pypz) has been one of the focuses for our group. A new derivative 1-benzoyl-3-(pyridine-2-yl)-1H-pyrazole (L) with *NNO* donor atoms was synthesized by introducing a benzoyl moiety to pypz [1]. Pyridine-pyrazole binds to metal centres through the N atoms which are relatively similar to bpy ligands. Besides, pypz compound is widely used as a ligand for transition metal complexes which are redox-active and, or exhibit interesting photoelectrochemical properties [2-7]. Ru(II) complexes based on bpy ligands have been intensively studied and used as photosensitiser in PEC applications [8-10]. The development and utilization of terpyridine and quaterpyridine ligands have improved the photocurrent and power conversion efficiencies by harvesting lower energy wavelengths particularly in the near-IR region [7, 11-14]. However, optimum redox properties were sacrificed as a result of this improvement. The LUMO in ruthenium pyridyl complexes is located at the π-accepting ligand. Therefore, it is only appropriate to vary the structure of the ligand to tune the electronic property of the complex.

The pyrazole rings have similar π orbitals just like those of pyridyl rings, while possessing higher lying π* orbital [6]. The benzoyl moiety acts as a 'molecular switch' to tweak the electronic property of the ligand by extending the delocalization of electrons and fine-tune the LUMO states via utilisation of functional substituent groups, i.e. CH_3 and Cl. The study described herein is aimed to provide an understanding of Ru(II) complex properties with the implementation of L ligand. The use of electron withdrawing (Cl) and donating (CH_3) substituent groups on the benzoyl moiety of L ligand was intended to provide a wider perspective of the ligands' functionality that is crucial in order to tap into the potential applications in ruthenium-based PEC reactors.

2.0 METHODOLOGY

2.1 General Instrumentation

The infrared (IR) vibrational frequencies of all samples were measured on Agilent Cary 630 equipped with a 5 bounce zinc selenide attenuated total reflectance (5 bounce ZnSe ATR) sampling accessary. UV-Vis spectra of samples dissolved in acetonitrile (CH_3CN) were collected with the UV-1650 PC SHIMADZU spectrophotometer. The mass-to-charge (m/z) ratio of gaseous Ru(II) complex ions were determined by Bruker Daltonic (MicroTOF Q) mass spectrometer with the following conditions: drying gas, aerosol (0.2 Bar), dry heater (180 °C) and capillary voltage (4500 V). The samples were prepared in CH_3CN. ^{1}H NMR spectra were obtained using 400 MHz JEOL/JNM-ECP spectrometer. Chemical shifts (δ) are reported in ppm against deuterated DMSO or acetone. The photoluminescence property of Ru(II)complexes were collected on FP-6600 JASCO spectroflourometer at room temperature (298 K) in CH_3CN solution through a 1 cm path length quartz cell and a 150 W xenon lamp. The photoluminescence quantum yield (Φ_s) was measured with the standard in the following equation:

$$\Phi_s = \Phi_{std} \times \frac{A_{std}}{A_s} \times \frac{I_s}{I_{std}} \times \frac{\eta_s^2}{\eta_{std}^2}$$

where Φ_{std} is the quantum yield of standard reference, $[Ru(bpy)_3][PF_6]_2$ (Φ_{std} = 0.094 at 298 K in CH_3CN) [15]. A_{std} and A_s are the integrated emission peak intensities of standard reference and sample. I_s and I_{std} are the intensity of optical excitation for sample and standard. η_s and η_{std} are the solvent reflective index used for sample and standard.

Full geometry optimization and electronic excitation properties were carried out using DFT and TDDFT methods, respectively, with B3LYP exchange-correlation functional and 6-31G (d,p) basis-set (H, C, N, O & Cl) and LAN2LDZ basis set as effective core potential (Ru). The vibrational frequency calculations were performed to ensure that the optimized geometries represent the local minima and there are only positive eigen values. All calculations were performed with Gaussian09 program package.

2.2 Synthesis and Characterisation of Ru(II) Complexes

All experiments were performed under an inert atmosphere of N_2 gas using Schlenk techniques. CH_3CN and triethylamine (Et_3N) were pre-dried with CaH_2 and distilled. Ethanol (EtOH) and were used as received and deoxygenated by bubbling with N_2 prior to usage.

Synthesis of 2-(1H-pyrazol-3-yl)pyridine (pypz), and $Ru(bpy)_2Cl_2$ ($RuCl_2$) were prepared based on previous methods [1, 2, 16, 17]. pypz: FT-IR (ATR, cm^{-1}): 3120; broad ν(NH), 1598-1589 ν(C=N). UV-Vis (nm, ε/L mol^{-1} cm^{-1}): 252, 15930 (π-π*); 285, 13054 (π-π*). ^{1}H-NMR (400 MHz, DMSO-D_6) δ 13.17 (s, 1H), 8.58 (d, 1H), 8.11-7.56 (m, 3H), 7.30 (t, 1H), 6.85 (d, 1H)

Synthesis of $[Ru(bpy)_2(pypz)](PF_6)_2$, abbreviated as Ru(pypz). The reaction of $RuCl_2$ with pypz in 1:1 ratio under refluxing condition in H_2O/EtOH for a period of 8 hours gave a Ru(II) complex ion with the general formula $[Ru(bpy)_2(pypz)]^{2+}$. The reaction mixture was allowed to cool to room temperature and the cationic complex was precipitated out by an addition of ammonium hexaflorophosphate, $[NH_4][PF_6]$. The solid product was filtered, washed with distilled water and then dried under vacuum. The crude complex is dissolved in CH_3CN and purified on a Sephadex LH-20 column with CH_3CN as the eluent. FT-IR (ATR, cm^{-1}) 1606 ν(C=N), 837 ν(PF) . ^{1}H-NMR (DMSO-D_6) δ 14.19 (s, 1H), 8.80 (d, 3H), 8.76 (d, 1H), 8.41 (d, 1H), 8.25-8.01 (m, 6H), 7.78-7.74 (d, 1H), 7.74-7.70 (d, 1H), 7.68 (d, 1H), 7.65-7.56 (m, 2H), 7.56-7.48 (m, 4H), 7.48-7.42 (t, 1H), 7.37 (t, 1H). *m/z* 704.02 $[Ru(bpy)_2(pypz)](PF_6)^+$ (calc. m/z = 704.07).

Synthesis of RuL, Ru(*m*-CH_3-L) and Ru(*m*-Cl-L). Ru(pypz) was dissolved in dry CH_3CN (20 ml) and Et_3N (1 ml) and stirred for 15 minutes. Then, benzoyl chloride was added into the solution and heated at 60^0C for 4 hours. Upon completion, the solvent was removed under reduced pressure. The crude RuL complex was dissolved in CH_3CN and purified on a Sephadex LH-20 column with CH_3CN as the eluent. The same procedure was repeated for the synthesis of Ru(*m*-CH_3-L) and Ru(*m*-Cl-L) with the use of 3-methylbenzoyl chloride and 3-chlorobenzoyl chloride reagent, respectively. RuL: FT-IR (ATR, cm^{-1}) 1728 *v*(C=O), 1604 *v*(C=N), 840 *v*(PF). ^{1}H-NMR (400 MHz, DMSO-D_6) δ 8.84 (t, J = 8.9 Hz, 2H), 8.64 (dd, 2H), 8.52 (d, 1H), 8.38-8.28 (m, 2H), 8.26-8.10 (m, 4H), 7.86-7.74 (m, 3H), 7.72-7.64 (m, 3H), 7.63-7.55 (m, 3H), 7.54-7.44 (m, 4H), 7.35-7.21 (m, 3H). *m/z* 808.04 $\{[Ru(bpy)_2(L)][PF_6]\}^+$ (calc. m/z = 808.10). Ru(*m*-CH_3-L): FT-IR (ATR, cm^{-1}) 1726 *v*(C=O), 1605 *v*(C=N), 822 *v*(PF). ^{1}H-NMR (Acetone-D_6) δ 8.83 (t, 2H), 8.65 (d, 2H), 8.59 (d, 1H), 8.47 (d, 1H), 8.33-8.15 (m, 5H), 7.99 (t, 2H), 7.94-7.80 (m, 3H), 7.75 (d, 2H), 7.62 (d, 2H), 7.53 (q, 2H), 7.43-7.30 (m, 2H), 7.20 (d, 1H), 7.16 (s, 1H), 2.33 (s, 3H). *m/z* 822.06 $\{[Ru(bpy)_2(m\text{-}CH_3\text{-}L)][PF_6]\}^+$ (calc. m/z = 822.11) Ru(*m*-Cl-L): FT-IR (ATR, cm^{-1}) 1731 *v*(C=O), 1605 *v*(C=N), 824 *v*(PF). ^{1}H-NMR (DMSO-D_6) δ 8.84 (t, 2H), 8.67 (s, 2H), 8.56 (s, 1H), 8.42 (d, 1H), 8.32 (d, 1H), 8.28-8.04 (m, 4H), 8.00-7.79 (3H), 7.79-7.41 (m, 9H), 7.31 (s, 3H). *m/z* 842.05 $\{[Ru(bpy)_2(m\text{-Cl-L})][PF_6]\}^+$ (calc. m/z = 842.06)

3.0 RESULTS AND DISCUSSION

3.1 Synthesis

The initial efforts to synthesise RuL via pathway I was unsuccessful (Figure 1.). Structural investigation of the desired Ru(II) complex with IR spectroscopy showed the absence of C=O stretching frequency. The presence of acetamide group, -N-C=O between the pypz fragment and the bz moeity posed a concern for the stability of the ligand. Acetamide group has the probability of undergoing hydrolysis via acid or base-catalysed reactions [18]. The reaction in Pathway I unintentionally provides a relatively favourable aqueous (H_2O/EtOH) medium for hydrolysis of acetamide bond. Consequently, we altered the reaction steps and favoured the addition of benzoyl chloride with the ionic complex Ru(pypz) at the final reaction step. Thereby, the use of H_2O/EtOH was avoided and, instead, CH_3CN was used for the reaction. As a result, complex RuL and subsequently Ru(*m*-CH_3-L) and Ru(*m*-Cl-L) were successfully synthesised via pathway II.

The strong C=O stretching frequency signal can be a very useful tool to observe the presence of benzoyl group as well as to gauge the electronic perturbation in the ligand. A strong IR frequency signal at 822-840 cm^{-1} for Ru(pypz), RuL, Ru(*m*-CH_3-L) and Ru(*m*-Cl-L) is attributed to the $[PF_6]^-$ counter ion. The broad NH vibration signal which is apparent in the IR spectrum of Ru(pypz) was absent in the RuL, Ru(*m*-CH_3-L) and Ru(*m*-Cl-L) that indicated the formation of acetamide group.

The ^{1}H NMR spectrum of the Ru(II) complexes were collected in either deuterated DMSO or acetone. The ^{1}H NMR spectra of both complexes are very difficult to interpret due to the presence of a large number of protons. The assignment of proton signals were made even more difficult with the overlapping of proton signals with chemically equivalent environments involved in the two bpy ligands, and *R*-L. Fortunately, the intergral of peaks corresponded to the actual number of protons present in the complexes. The most significant signal found for Ru(pypz) is the appearance of a far downfield singlet N-H peak at 14.19 ppm that

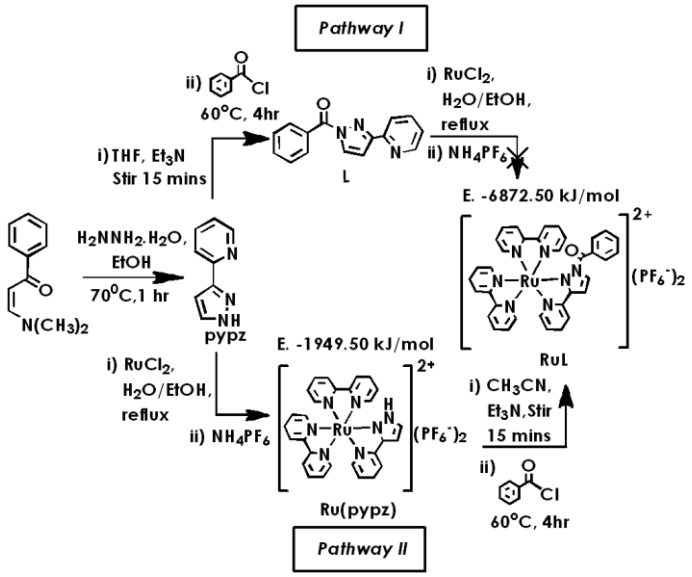

Figure 1 Schematic diagram showing two possible pathways for RuL synthesis

belongs to the pyrazole ring. This peak is also shifted downfield by ~1.02 ppm as compared to the free pypz ligand (δ_{NH} 13.17).

The calculated (DFT) energy of formation for RuL (ΔE_f = -6872.50 kJ/mol) is approximately three-fold in magnitude in comparison to Ru(pypz) (ΔE_f = -1949.50 kJ/mol). This result suggests that the attachment of pendant benzoyl fragment lead to the extra stability of RuL.

3.2 Electronic Structure

In the case of RuL, a total of 804 orbitals were involved in the Mulliken population analysis with 308 electrons involved and distributed over 154 occupied molecular orbitals. The rest of the 650 orbitals constitute the unoccupied molecular orbitals. The electron distributions for the six frontier orbitals of occupied and unoccupied molecular orbitals (MO)s involved in the ruthenium complex are shown in Figure 2. The first three HOMOs (HOMO, HOMO-1 and HOMO-2) are concentrated 3-dimensionally on the ruthenium metal centre. On the other hand, the frontier LUMO orbitals (LUMO, LUMO+1 and LUMO+2) demonstrated a progression of energy line-up with the LUMO (-2.65 eV) coming from L ligand and next in line (LUMO+1) is one of the bpy ligand with an energy separation of 0.11 eV. LUMO+2 comes from the other bpy ligand (-2.41 eV). Therefore, the L ligand is now responsible for the fine-tuning of LUMO energy level with the introduction of substituent group (CH_3 and Cl) on the benzoyl moiety [19]. In a heterogeneous TiO_2-based PEC system, the Ru(II) photosensitiser exhibits a metal [Ru(II)] to ligand charge transfer (MLCT) band in which the ligands participated in the injection of photoexcited electrons into TiO_2 [20]. Therefore, based on the DFT calculated molecular orbitals, the Ru(II) photosensitiser is expected to possess a similar observation since the occupied states originate from the ruthenium centre and the empty states are located on the ligands

3.3 Photoluminescence and Band Energy Studies

Herein, Ru(II) complexes with electron withdrawing (e.g. Cl) and donating (e.g. CH_3) substituent groups at the meta position of the benzoyl moiety were chosen along with unsubstituted RuL to represent the different effects of substituent groups on the emission properties. Excitation, emission wavelengths and respective quantum yields of Ru(II) complexes are listed in Table 1. Initially, ground state (^{1}GS) singlet electron was excited from HOMO (metal) to LUMO (*R*-L) descrided as the

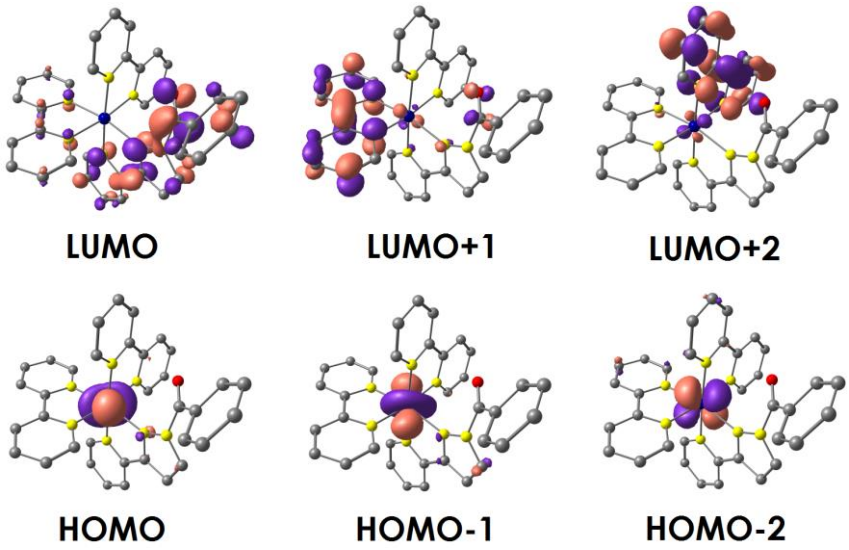

Figure 2 Isosurface plot (contour value = 0.052) of the first three frontier HOMO and LUMO for RuL.

Table 1 Experimental and calculated emission data for RuL, Ru(*m*-CH_3-L) and Ru(*m*-Cl-L) measured in CH_3CN.

Complex	Excitation wavelength (λ_{ex}/nm)	Emission Wavelength (λ_{em}/nm)	Quantum yield[a] (Φ_S)	^{3}MLCT[b] (eV)
RuL	444	628	0.0076	-3.63
Ru(*m*-CH_3-L)	442	630	0.0023	-3.62
Ru(*m*-Cl-L)	448	630	0.0191	-3.71

[a] $Ru(bpy)_3Cl_2$ (Φ_r = 0.094 in CH_3CN) as reference compound
[b] Calculated energy level

MLCT singlet electron transition (^{1}MLCT) (Figure 3.). Then, the excited singlet electron undergoes non-radiative relaxation via intersystem crossing (ISC) where the spin of the excited electron is reversed to a triplet state, ^{3}MLCT. Finally, the excited electrons of ^{3}MLCT eventually relaxes radiatively back to the ground state. The singlet-triplet energy gap was obtained by substrating the triplet energy state from the energy of singlet state.

Also present is the metal-centred (^{3}MC) triplet state which has energies comparable to that of the MLCT states. Energy spacing, ΔE found between ^{3}MLCT and ^{3}MC determines the thermal accessibility of excitedelectrons into the upper ^{3}MC. Smaller ΔE reflects higher population of ^{3}MC state. The relative energy ordering of ^{3}MLCT-^{3}MC was altered by variation of the substituent on the bz moiety [21]. However, ^{3}MC states are relatively independent of the substituents used for the mentioned purpose [22].

Figure 4. shows the calculated energy gap of triplet state (^{3}MLCT) and the ground state HOMO for RuL, Ru(*m*-CH$_3$-L) and Ru(*m*-Cl-L). RuL, Ru(*m*-CH$_3$-L) and Ru(*m*-Cl-L) demonstrated an increasing quantum yield trend as follows, Ru(*m*-CH$_3$-L) (Φ_s = 0.0023) < RuL (Φ_s = 0.0076) < Ru(*m*-Cl-L) (Φ_s = 0.0191). Ru(*m*-CH$_3$-L) has the highest calculated ^{3}MLCT energy level (-3.62 eV) that narrowed the ΔE of ^{3}MLCT and ^{3}MC. Inevitably, increases the thermal accessibility of ^{3}MC state from the ^{3}MLCT state. Eventually, photo-excited electrons in the upper ^{3}MC irreversibly undergo non-radiative decay back to the ground state and/or to photoproducts. Meanwhile, Ru(*m*-Cl-L) has the lowest ^{3}MLCT energy level, thus avoid the thermal accessibility of ^{3}MC $\rightarrow$ ^{3}MLCT and improved the radiative emissions. As a result, Ru(*m*-Cl-L) and Ru(*m*-CH$_3$-L) have the highest and the lowest photoluminescence quantum yield, respectively.

An effective Ru(II) photosensitiser for a PEC water splitting reaction should have LUMO (in this case, the long-lived ^{3}MLCT state) energy level higher than the conduction band of TiO_2 (-4.00 eV; CH_3CN), to drive photoexcited electrons into the latter [23]. Narrowing of the ^{3}MLCT and TiO_2 conduction band could also improve the electronic injection process [24]. Based on Figure 4, Ru(*m*-Cl-L) has a better leverage on improving injection of its photoexcited electrons into TiO_2, since its ^{3}MLCT energy level is comparatively the lowest and closes to the conduction band of TiO_2. Besides, Ru(*m*-Cl-L) would also have more photoexcited electrons in participation compared to RuL and Ru(*m*-CH$_3$-L), which is reflected by the high photoluminescence quantum yield value and indirectly improve the overall photocurrent generation efficiency for PEC applications. Furthermore, Ru(*m*-Cl-L) has the narrowest calculated HOMO-^{3}MLCT (2.45 eV) that corresponds to its ability to harvest longer wavelengths energies. The solar absorption of Ru(II) complexes could be extended across the visible and into near IR spectrum of light with systematic use of stronger electron withdrawing substituents.

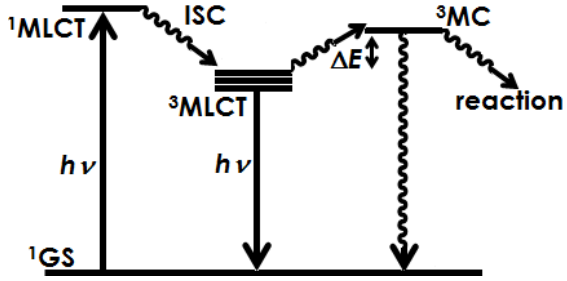

Figure 3 Simplified Jablonski diagram for Ru(II) complex. The energy spacing (ΔE) of ^{3}MLCT and ^{3}MC controls the thermal accessibility of ^{3}MC state.

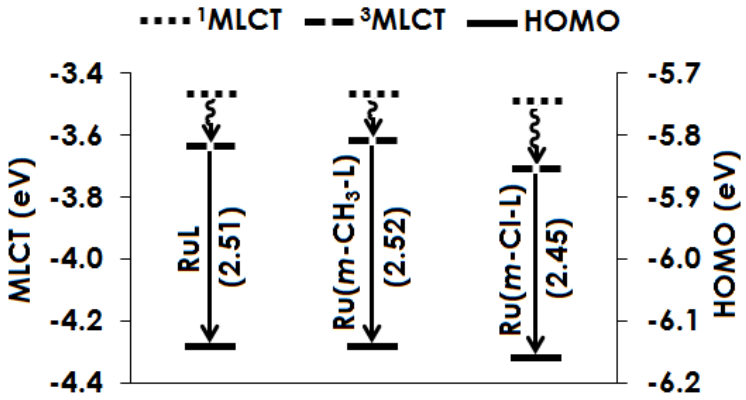

Figure 4 Calculated singlet to triplet emission data for Ru(*m*-CH$_3$-L), RuL and Ru(*m*-Cl-L) measured in CH_3CN. The energy gap of ^{3}MLCT and ground state HOMO is given in parenthesis.

4.0 CONCLUSION

Highly versatile bis(bipyridyl)-Ru(II)-1-benzoyl-3-(pyridine-2-yl)-1H-pyrazole and derivative complexes were successfully synthesised and characterised. The implementation of CH_3 and Cl substituent groups on the benzoyl moiety has successfully tuned the LUMO energy level of complex that is capable of harvesting longer wavelength energies and to match the conduction band of TiO_2 photocatalyst. Ruthenium(II) complex particularly Ru(*m*-Cl-L) has the potential to be applied as photosensitiser in PEC systems due to its comparatively higher photoluminescence quantum yield and possesses a MLCT energy level that is comparable to the conduction band of TiO_2.

Acknowledgement

The Authors would like to acknowledge the Ministry of Science & Technology (MOSTI) and Ministry of Education (MOE) Malaysia for sponsoring this project under 06-01-02-SF1001 and ERGS/1/2013/TK07/UKM/02/2, respectively. Special thanks to Prof. Hideaki Kasai and JASSO for a research attachment (to Mark-Lee) under the Quantum Engineering Design Course (QEDC) at Osaka University (2014-2015). Sincere gratitude to Prof. Wilson Agerico Diño, Prof. Makoto Yasuda and School of Chemical Sciences and Food Technology, UKM for their relentless support and provision of experimental facilities.

References

[1] Shelton, A. H., Stephenson, A., Ward, M. D. and Kassim, M. B. 2011. 1-Benzoyl-3-(pyridin-2-yl)-1H-pyrazole. *Acta Crystallographica Section E*. 67(9): o2445-o2445.

[2] Adams, H., Alsindi, W. Z., Davies, G. M., Duriska, M. B., Easun, T. L., Fenton, H. E., Herrera, J. M., George, M. W., Ronayne, K. L., Sun, X. Z., Towriec, M and Ward, M. D. 2006. New Members of the $[Ru(diimine)(CN)_4]^{2-}$ Family: Structural, Electrochemical and Photophysical Properties. *Dalton Transactions*. 1: 39-50.

[3] Bozoglian, F., Romain, S., Ertem, M. Z., Todorova, T. K., Sens, C., Mola, J., Rodríguez, M., Romero, I., Benet-Buchholz, J., Fontrodona, X., Cramer, C. J., Gagliardi, L. and Llobet, A. 2009. The Ru-Hbpp Water Oxidation Catalyst. *Journal of the American Chemical Society*. 131(42): 15176-15187.

[4] Colombo, A., Dragonetti, C., Magni, M., Meroni, D., Ugo, R., Marotta, G., Grazia Lobello, M., Salvatori, P. and De Angelis, F. 2015. New Thiocyanate-free Ruthenium(II) Sensitizers with Different Pyrid-2-yl Tetrazolate Ligands for Dye-sensitized Solar Cells. *Dalton Transactions*. 44(26): 11788-11796.

[5] Huang, J-F., Liu, J-M., Su, P-Y., Chen, Y-F., Shen, Y., Xiao, L-M., Kuang, D.-B. and Su, C.-Y. 2015. Highly Efficient and Stable Cyclometalated Ruthenium(II) Complexes as Sensitizers for Dye-sensitized Solar Cells. *Electrochimica Acta*.174: 494-50.

[6] Klein, C., Baranoff, E., Grätzel, M. and Nazeeruddin, M. K. 2011. Convenient Synthesis of Tridentate 2,6-di(pyrazol-1-yl)-4-carboxypyridine and Tetradentate 6,6'-di(pyrazol-1-yl)-4,4'-dicarboxy-2,2'-bipyridine Ligands. *Tetrahedron Letters*. 52(5): 584-587.

[7] Wu, G., Kaneko, R., Zhang, Y., Shinozaki, Y., Sugawa, K., Islam, A., Han, L., Bedja, I., Gupta, R. K., Shen, Q. and Otsuki, J. 2016. Neutral and Anionic Tetrazole-Based Ligands in Designing Novel Ruthenium Dyes for Dye-Sensitized Solar Cells. *Journal of Power Sources*. 307: 416-425.

[8] Maeda, K., Sahara, G., Eguchi, M. and Ishitani, O. 2015. Hybrids of a Ruthenium(II) Polypyridyl Complex and a Metal Oxide Nanosheet for Dye-Sensitized Hydrogen Evolution with Visible Light: Effects of the Energy Structure on Photocatalytic Activity. *American Chemical Society Catalysis*. 5(3): 1700-1707.

[9] Li, F., Fan, K., Wang, L., Daniel, Q., Duan, L. and Sun, L. 2015. Immobilizing Ru(Bda) Catalyst on a Photoanode Via Electrochemical Polymerization for Light-Driven Water Splitting. *American Chemical Society Catalysis*. 5(6): 3786-3790.

[10] Vougioukalakis, G. C., Philippopoulos, A. I., Stergiopoulos, T. and Falaras, P. 2011. Contributions to the Development of Ruthenium-Based Sensitizers for Dye-Sensitized Solar Cells. *Coordination Chemistry Reviews*. 255(21-22): 2602-2621.

[11] Funaki, T., Funakoshi, H., Kitao, O., Onozawa-Komatsuzaki, N., Kasuga, K., Sayama, K. and Sugihara, H. 2012. Cyclometalated Ruthenium(II) Complexes as Near-IR Sensitizers for High Efficiency Dye-Sensitized Solar Cells. *Angewandte Chemie-International Edition*. 51(30): 7528-7531.

[12] Nazeeruddin, M. K., Péchy, P., Renouard, T., Zakeeruddin, S. M., Humphry-Baker, R., Cointe, P., Liska, P., Cevey, L., Costa, E., Shklover, V., Spiccia, L., Deacon, G. B., Bignozzi, C. A. and Grätzel, M. 2001. Engineering of Efficient Panchromatic Sensitizers for Nanocrystalline TiO_2-Based Solar Cells. *Journal of the American Chemical Society*. 123(8): 1613-1624.

[13] Renouard, T., Fallahpour, R. A., Nazeeruddin, M. K., Humphry-Baker, R., Gorelsky, S. I., Lever, A. B. P. and Grätzel, M. 2002. Novel Ruthenium Sensitizers Containing Functionalized Hybrid Tetradentate Ligands: Synthesis, Characterization, and INDO/S Analysis. *Inorganic Chemistry*. 41(2): 367-378.

[14] Barolo, C., Nazeeruddin, K., Fantacci, S., Censo, D. Di, Comte, P., Liska, P., Viscardi, G., Quagliotto, P., De Angelis, F., Ito, S., Gra, M., Lausanne, D., Lausanne, C., Cnr, I., Uni, V., Elce, V. and Perugia, I. 2006. Synthesis, Characterization, and DFT-TDDFT Computational Study of a Ruthenium Complex Containing a Functionalized Tetradentate Ligand. *Inorganic Chemistry*. 45(12): 4642-4653.

[15] Suzuki, K., Kobayashi, A., Kaneko, S., Takehira, K., Yoshihara, T., Ishida, H., Shiina, Y., Oishi, S. and Tobita, S. 2009. Reevaluation of Absolute Luminescence Quantum Yields of Standard Solutions Using a Spectrometer with an Integrating Sphere and a Back-Thinned CCD Detector. *Physical Chemistry Chemical Physics*. 11(42): 9850-9860.

[16] Jones, P. L., Amoroso, A. J., Jeffery, J. C., McCleverty, J. a., Psillakis, E., Rees, L. H. and Ward, M. D. 1997. Lanthanide Complexes of the Hexadentate N-Donor Podand Tris[3-(2-pyridyl)pyrazolyl]hydroborate: Solid-State and Solution Properties. *Inorganic Chemistry*. 36(1): 10-18.

[17] Sullivan, B. P., Salmon, D. J. and Meyer, T. J. 1978. Mixed Phosphine 2,2'-Bipyridine Complexes of Ruthenium. *Inorganic Chemistry*: 17(12): 3334-3341.

[18] Hori, K., Ikenaga, Y., Arata, K., Takahashi, T., Kasai, K., Noguchi, Y., Sumimoto, M., and Yamamoto, H. Theoretical Study on the Reaction Mechanism for the Hydrolysis of Esters and Amides under Acidic Conditions. *Tetrahedron*. 63(5): 1264-1269.

[19] Medlycott, E. A. and Hanan, G. S. 2005. Designing Tridentate Ligands for Ruthenium (II) Complexes with Prolonged Room Temperature Luminescence Lifetimes. *Chemical Society reviews*. 34(2): 133-142.

[20] Arifin, K., Majlan, E. H., Wan Daud, W. R. and Kassim, M. B. 2012. Bimetallic Complexes in Artificial Photosynthesis for Hydrogen Production: A Review. *International Journal of Hydrogen Energy*. 37(4): 3066-3087.

[21] Cherry, W. R. and Henderson, L. J. 1984. Relaxation Processes of Electronically Excited States in Polypyridine Ruthenium Complexes. *Inorganic Chemistry*. 23(22): 983-986.

[22] Wagenknecht, P. S. and Ford, P. C. 2011. Metal Centered Ligand Field Excited States: Their Roles in the Design and Performance of Transition Metal Based Photochemical Molecular Devices. *Coordination Chemistry Reviews*. 255(5-6): 591-616.

[23] Fan, W., Tan, D. and Deng, W. 2011. Theoretical Investigation of Triphenylamine Dye/Titanium Dioxide Interface for Dye-Sensitized Solar Cells. *Physical Chemistry Chemical Physics : PCCP*. 13(36): 16159-16167.

[24] Hara, K., Sato, T., Katoh, R., Furube, A., Ohga, Y., Shinpo, A., Suga, S., Sayama, K., Sugihara, H. and Arakawa, H. 2003. Molecular Design of Coumarin Dyes for Efficient Dye-Sensitized Solar Cells. *J. Phys. Chem. B*. 107(2): 597-606.